J Biochem Technol (2023) 14(4): 83-89
https://doi.org/10.51847/jIOvZK4SgJ
ISSN: 0974-2328

# Purification of Phosphoric Acid Solution Using Natural and Activated Clays

**Chedlia Mhedhbi, Mahjoub Jabli, Nabil Mabrouki, Mustapha Hidouri, Khaled Boughzala***

Received: 14 September 2023 / Received in revised form: 30 November 2023, Accepted: 04 December 2023, Published online: 16 December 2023

## Abstract

Phosphoric acid ($H_3PO_4$), commonly derived from phosphate rock, is vital in industry as it could be employed in numerous processes. Several techniques were used to purify $H_3PO_4$. In the current work, natural and $H_2SO_4$-activated clays were used to reduce cadmium (Cd) and magnesium (Mg) ions from the $H_3PO_4$ solution through the adsorption method. The solid materials were characterized using several analytical methods including Elemental analysis, Scanning Electron Microscopy (SEM), Fourier Transform Infrared (FT-IR) spectroscopy, X-ray diffraction (XRD), Brunauer-Emmett-Teller (BET), and Thermogravimetric analysis (TGA-DTA). The main constituents of the studied clays were $SiO_2$ (43.64 - 51.24 %), and $Al_2O_3$ (19.92 – 31.24%). The specific surface area values of the studied clays ranged from 74.25.35 to 85.14 $m^2/g$. The diffractograms showed the presence of kaolinite, quartz, goethite, and hematite. Clay micrographs were formed of agglomerates with irregular shapes and small sizes (1 - 3 µm). The cadmium and magnesium retention capacity in clays are higher than 50% and 36%, respectively. The adsorption process followed well pseudo-second kinetic order and Freundlich isotherm equations. The process is demonstrated to be chemical. Overall, the current study has confirmed the efficiency of using abundant natural clays and activated ones to reduce Cd and Mg ions in phosphoric acid solution.

**Keywords:** Phosphoric acid, Activated clays, Adsorption, Magnesium, Cadmium

**Chedlia Mhedhbi**
Higher Institute of Technological Studies of Ksar Hellal, 5070 Ksar-Hellal, Tunisia.

**Mahjoub Jabli**
Department of Chemistry, College of Science, Majmaah University, Al-Majmaah, 11952, Saudi Arabia.
Textile Materials and Processes Research Unit, Tunisia National Engineering School of Monastir, University of Monastir, Tunisia.

**Nabil Mabrouki**
Laboratory of Physical-chemistry of Materials, Faculty of Sciences of Monastir, 5019 Monastir, Tunisia.

**Mustapha Hidouri**
Research laboratory: Energy, Water, Environment and Processes, LREWEP (LR18ES35), National Engineering School of Gabes, University of Gabes, 6072 Gabes, Tunisia.

**Khaled Boughzala***
Higher Institute of Technological Studies of Ksar Hellal, 5070 Ksar-Hellal, Tunisia.
Laboratory of Physical-chemistry of Materials, Faculty of Sciences of Monastir, 5019 Monastir, Tunisia.

***E-mail:** khaledboughzala@gmail.com

## Introduction

Natural phosphorus compounds are of crucial importance for the production of phosphate fertilizers which are necessary for global agriculture (Becker, 1989; Toama, 2017). Two main geological origins exist for phosphate ores: sediment and igneous (Becker, 1989). $H_3PO_4$ is an intermediate chemical substance. Several methods were developed to produce $H_3PO_4$ (Becker, 1989; Kthiri *et al*., 2022). The most widely used method is the wet process, due to its low price and energy consumption (Delcea & Siserman, 2021; Delcea *et al*., 2023c). Natural phosphate is dissolved by mineral acids, which could contaminate the product with several heavy metals (Delcea *et al*., 2023a, 2023b). Nitric acid, sulfuric acid, or hydrochloric acid are used to dissolve phosphate. In terms of volume, wet digestion of phosphate rock using $H_2SO_4$ is the preferred method (European Commission, 2007).

Phosphoric acid can be used to make phosphate fertilizers and manufacture food additives due to bond purity regulations, detergents for the pharmaceutical industry, paints, and cosmetics (Delcea *et al*., 2023b). It is also used for the treatment of wastewater, pickling, polishing, and antirusting of metal surfaces (Gonzalez *et al*., 2002). However, heavy metals and other dissolved impurities in phosphate material could contaminate the final product during the production of phosphoric acid. Therefore, these heavy metals may contaminate phosphorus fertilizers which would then spread to the soil and atmosphere. The growing environmental levels of heavy metals pose a major hazard to human health, living things, and ecological systems (Inglezakis *et al*., 2018; Saleh & Ali, 2018). The purification of phosphoric acids is so necessary. Thus, the design of an effective technique to eliminate impurities that contaminate $H_3PO_4$ is necessary for the sustainable production of phosphate fertilizers from wet $H_3PO_4$. The presence of contaminants including organic waste and heavy metals that were initially present in phosphate rocks is one of the main downsides of wet $H_3PO_4$ manufacturing. Indeed, cadmium is a minor component in phosphate rock. It is a contaminant. Depending on the deposit, ores containing between 10 and 80 g/ton cadmium may be discovered in both phosphoric acid and phosphate fertilizers. The amount of cadmium brought by phosphate fertilizers depends on the origin of the phosphates used

during manufacturing. The World Health Organization (WHO) describes cadmium as a dangerous element that may build up in soils and plants, leak into ground and surface waters, enhance crop absorption, increase levels in animals and food, and could be harmful to human health (Zhao *et al*., 2017).

Calcination is an efficient way to remove cadmium from raw phosphate, but it needs temperatures between 850°C and 1150°C. It is not thought to be cost-effective (Boughzala & Hidouri, 2020). Several techniques, such as solvent extraction, adsorption, ion exchange, precipitation, flotation, and membrane processes, have been developed to remove cadmium from phosphoric acid solutions. Magnesium ion, found in $H_3PO_4$, causes a variety of issues such as worsening acid viscosity, raising operational complexity, operating costs, and decreasing fertilizer water solubility (Boughzala & Hidouri, 2020; Bembli *et al*., 2022). Therefore, $Mg^{2+}$ ion removal from $H_3PO_4$ will be crucial for practical production.

The present work focuses on the use of abundant natural and $H_2SO_4$-activated clays to remove cadmium and magnesium ions from a phosphoric acid solution. The solid materials were characterized using Elemental analysis, SEM, FT-IR spectroscopy, XRD and BET. The adsorption process was assessed by varying experimental conditions. The kinetic and isotherm data were modeled using common theoretical kinetic and isotherm equations.

## Materials and Methods

*Natural Phosphate Preparation*

Oum El Khecheb (Gafsa–Metlaoui) deposit is an old mine in the South of Tunisia. The most mineralized and possibly lucrative strata, according to the mineralogical investigation, are layers CII, CV, CVI, and CVIII. Despite having relatively high amounts of MgO and Cd, analyses of the phosphate from CII they were revealed that the deposit has a major economic interest due to its high proportion of $P_2O_5$. Phosphate was subjected to crushing, washing, and desliming to obtain fine particles. Particles have been thoroughly washed with distilled water before use and then dried in an oven at 105°C.

*Preparation of Activated Clays*

Different types of clays, collected from Nafta and Tozeur regions (south of Tunisia) were studied in this work. To prepare activated clays, the minerals were subjected to chemical treatments in 5 M sulphuric acid (>95% Prolabo) (10 g/500 mL) at 80°C for 2 h under magnetic stirring. After, the clays were washed with deionized water until the water became neutral. Then, the activated minerals were dried in a drying oven at 105°C. In the following sections, the mineral clays collected from Nafta, Tozeur, and acid-treated clays of Nafta will be labeled as RBC, ABC, and ACHTC (Ta), respectively.

*Production of Phosphoric Acid*

As previously said, the majority of phosphate rock is converted into phosphoric acid via a wet method. Apatite, which makes up the majority of phosphate rock, reacts with concentrated $H_2SO_4$ to produce phosphoric acid and an insoluble calcium sulfate salt. This process facilitates the direct filtration separation of phosphoric acid.

The following reaction shows the entire $H_2SO_4$ attack for producing phosphoric acid (Toama, 2017).

$$Ca_{10}(PO_4)_6F_2 + 10H_2SO_4 + 20H_2O \rightarrow 6H_3PO_4 + 10CaSO_4.\ 2H_2O + 2HF$$

A variety of phosphate rocks can be processed using the dihydrate method, and the weak acid comprises 26–30% $P_2O_5$. This weak acid is then evaporated to a concentration of 50–54% to fulfill the needs of fertilizer manufacturers.

*Adsorption Experiments*

The removal of cadmium and magnesium ions was carried out using natural and acid-activated clays as adsorbents. The adsorbent dosage was varied from 0.02 and 0.1g. The adsorption of different ions was performed in a batch mode, at room temperature, shaking speed of 150 rpm, using 20 mL of phosphoric acid solution. Ions concentrations were prepared by the dilution of stock solution

The adsorbed quantity ($q_e$, mg/g) was determined using the following equation:

$$q_e = (C_0 - C_e) \times {}^{V}/_{m} \quad (1)$$

V is the utilized solution volume (L), m is the mass of the clay material (mg), and $C_0$ and $C_e$ correspond to the initial and equilibrium concentrations of Cd or Mg (mg/L), respectively.

*Characterization*

An atomic absorption spectroscopy (Perkin-Elmer 3110) was used to determine the chemical elements in natural phosphate as well as contaminants in phosphoric acid. The chemical compositions of the natural and activated clays were determined by X-ray fluorescence spectrometry (X-ray fluorescence spectrometer, Philips brand, and model PW-2400 equipped with a 3Wh power tube). An X'Pert Pro, PANalytical diffractometer running on Cu K□ radiation was used to perform powder XRD analysis. Using the information provided in the ASTM cards, the mineral phases were identified. A Perkin-Elmer 1283 spectrometer and the KBr pellet method were used to obtain Fourier transform infrared (FTIR) spectra. Using a Seteram Instrumentation SETSYS evolution system with a heating rate of 10°C/min up to 1000°C in an air atmosphere, thermal gravimetric analysis was carried out. Scanner Electronic Microscopy (SEM, FEI Quanta 200) was used to analyze the samples' surface morphology. BET (Brunauer-Emmett-Teller) equation was used to derive the specific surface area values from the nitrogen adsorption isotherms.

## Results and Discussion

*Characterization of Natural and Acid-Treated Clays*

The chemical analysis of the studied clays. The main constituents of these samples are $SiO_2$ (43.64 - 51.24 %), and $Al_2O_3$ (19.92 – 31.24%). Other elements are also found such as CaO (0.92 - 3.78

%), $Fe_2O_3$ (4.92-8.34 %), sodium oxide (0.25 – 1.47 %), and MgO (0.01 – 2.34 %). A high CaO content (3.78 %) is present in clay ACHTC (Ta). The clay samples exhibit a low percentage of MnO (0.04 - 0.13 %).

The specific surface area values of the studied samples range from 74.25.35 to 85.14 $m^2/g$. These values prove that these materials are non-porous. This trend aligns with the results of some other natural clay minerals studied in the literature (Bembli *et al*., 2022, Sboui *et al*., 2022).

The size and the shape vary and depend on the nature of the clay. Overall, the morphological behavior of all samples showed a clear resemblance. The agglomerates exhibit irregular shapes and small sizes ranging from 1 to 3 µm. These findings suggest that the morphology of clay powders influences the adsorption mechanism, which is suggested to be more favored when the powders are formed from more developed agglomerates. The diffractograms show the presence of kaolinite, quartz, goethite, and hematite. All samples present many phases, with quartz being the most prevalent one. This mineral is characterized by their basal reflections at 28.04 and 49.14°, respectively.

The results show, in addition to the above-mentioned constituents detected by XRD, the presence of a small amount of organic matter, in the form of compounds of aliphatic chains, characterized by the weak bands located at approximately 2920 and 2843 $cm^{-1}$. The deformation vibrations of Si-O-Mg and C-O bonds in carbonates are observed at 539 and 1450 $cm^{-1}$, respectively.

The bands at 3620-915 $cm^{-1}$ show the predominance of dioctahedral smectite with bands of [Al, Al-OH] (European Commission, 2007). The adsorption bands at 3430-1635 $cm^{-1}$, which correspond to the adsorbed water molecule on the clay surface, are assigned to the OH frequencies. The strong absorption bands observed at 1100 and 1000 $cm^{-1}$ are attributed to the silicate structure.

*Effect of Experimental Parameters on the Adsorption of Mg and Cd Ions from Phosphoric Acid*

**Table 1** displays the contents of $P_2O_5$, MgO, and Cd in diluted and concentrated $H_3PO_4$. Results reveal that the content of these elements is more important in the case of the diluted acid compared to the concentrated one.

**Table 1.** Contents of $P_2O_5$, MgO, and Cd in diluted and concentrated $H_3PO_4$

| Elements | $P_2O_5$ (%) | MgO (%) | Cd (ppm) |
|---|---|---|---|
| **Diluted $H_3PO_4$** | 43,2 | 2,9 | 41,75 |
| **Concentrated $H_3PO_4$** | 27,14 | 2,04 | 26,15 |

The effect of the adsorbent dosage on the adsorption of Mg and Cd ions is given in **Figure 1**. As it is observed, when the mass of the clay increases from 0 to 0.08 g, the adsorption efficiency of Cd ions for RBC clay increases from 0% to 57.6%. Further mass increase, (from 0.08 g to 0.1g), no effect is observed. However, the adsorption efficiencies of Cd ions for ABC and ACHTC (Ta) clays are 46.3% and 31.3%, respectively **(Figure 1a)**. At optimum masses of clays, the adsorption of Mg ions for ABC, RBC, and ACHTC (Ta) are 46.5%, 28.5, and 16.7%, respectively **(Figure 1b)**.

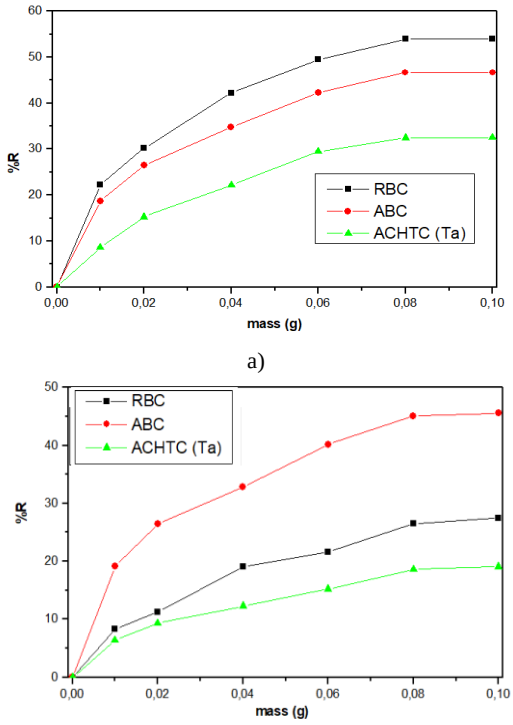


**Figure 1.** Effect of dosage mass of clay samples on the removal of a) Cd, b) Mg ions

The effect of contact time on the adsorption of Cd and Mg ions using the studied clays is shown in **Figure 2**. As contact duration increases, the adsorption of Cd and Mg ions increases and eventually reaches a plateau after about 20 min for the Cd and Mg ions. This phenomenon can be interpreted by the fact that there were a lot of sites accessible for Cd and Mg metals at the beginning of the reaction. Near equilibrium, there are fewer sites available, so difficult to access. Additionally, the rate of adsorption is reduced by the repulsive forces between the cations and the solid as well as those in the solution (Wang *et al*., 2015; Boughzala & Hidouri, 2020; Gmati *et al*., 2022; Bembli *et al*., 2024).

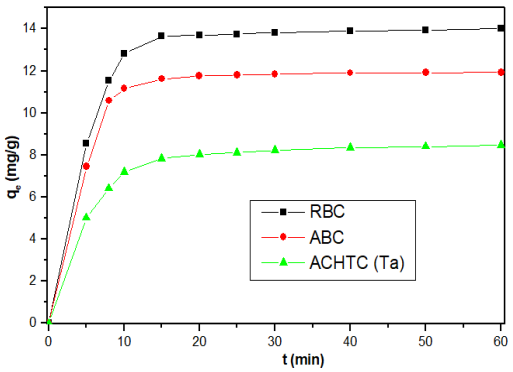

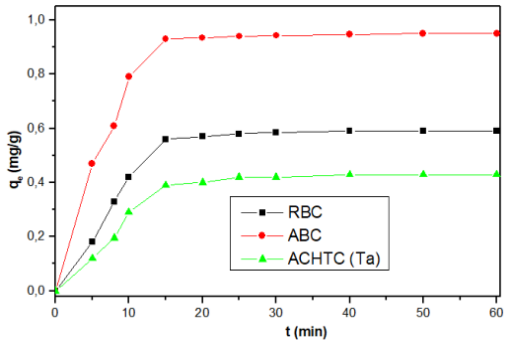


b)

**Figure 2.** Effect of contact time on the adsorption of a) Mg, b) Cd ions onto clay samples

**Figure 3** shows the change in the adsorbed capacity of Cd and Mg ions, as a function of phosphoric acid concentration, in the presence of the studied clays. It is observed that, at lower phosphoric acid concentrations, the adsorbed quantities of Cd and Mg ions increase significantly as $H_3PO_4$ concentration increases and further reaches stable values. This is assigned to the saturation of accessible sites on the surface of the studied clays at high $H_3PO_4$ concentration. For the RBC clay sample, the maximum adsorption capacity of Cd ions is 17.8 mg/g. However, the maximum adsorbed quantities of Cd ions for ABC and ACHTC (Ta) samples are 15.2 mg/g, and 11.8 mg/g, respectively. This difference in adsorption capacity is related to the change in the structural composition of the studied clays.

Similarly, **Figure 3b** gives the variation of the adsorbed quantity of Mg ions versus $H_3PO_4$ concentration. The adsorbed amounts of Mg ions for ACHTC (Ta) and RBC are 0.35 mg/g and 0.51 mg/g, respectively. The adsorption capacity is more important for the RBC clay sample, (0.92 mg/g). Indeed, the changes in the materials' surfaces and the availability of binding sites for the cadmium and magnesium metals are responsible for this difference in the adsorption efficiency.

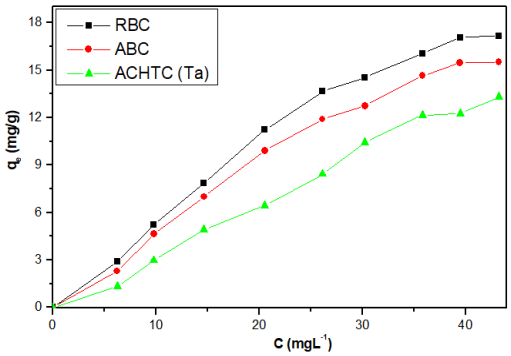


a)

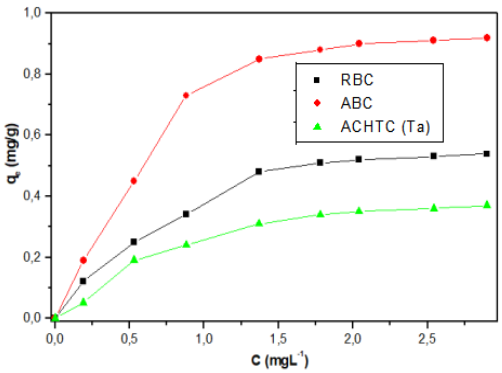


b)

**Figure 3.** Variation of the adsorbed amounts of **a**) Cd, b) Mg ions versus phosphoric acid concentration

*Kinetic Modeling*

The pseudo-first-order, pseudo-second-order, Elovich, and intra-particle diffusion models are used to simulate the equilibrium data (Ho & McKay, 1999; Bezzi *et al*., 2001; Ho *et al*., 2005; Bembli *et al*., 2021). **Table 2** summarizes the Kinetic parameters of Cd and Mg ions adsorption onto clay samples.

**Table 2.** Kinetic parameters of Cd and Mg ions adsorption onto clay samples

| | Cd | | | Mg | | |
|---|---|---|---|---|---|---|
| | **BBC** | **ABC** | **ACHT (Ta)** | **BBC** | **ABC** | **ACHT(Ta)** |
| **Pseudo first order** | | | | | | |
| **K** | 1.186 | 1.416 | 1.227 | 2.111 | 1.941 | 2.113 |
| **$q_e$** | 0.0566 | 0.0539 | 0.0539 | 0.146 | 0.207 | 0.103 |
| **$R^2$** | 0.722 | 0.862 | 0.744 | 0.961 | 0.979 | 0.962 |
| **Pseudo second order** | | | | | | |
| **K** | 0.038 | 0.055 | 0.041 | 0.206 | 0.283 | 0.200 |
| **$q_e$** | 14.535 | 12.312 | 8.772 | 0.686 | 1.024 | 0.523 |
| **$R^2$** | 0.999 | 0.999 | 0.999 | 0.995 | 0.997 | 0.994 |
| **Elovich** | | | | | | |
| □ | 150.139 | 309.74 | 41.949 | 0.196 | 0.988 | -0.0164 |
| □ | 0.575 | 0.755 | 0.812 | 6.498 | 5.558 | 8.071 |
| **$R^2$** | 0.826 | 0.783 | 0.909 | 0.883 | 0.861 | 0.824 |

| | | | | | | |
|---|---|---|---|---|---|---|
| **Intra Particular Diffusion** | | | | | | |
| **$K_t$** | 0.681 | 0.512 | 0.498 | 0.0614 | 0.0713 | 0.05 |
| **C** | 9.683 | 8.727 | 5.2 | 0.204 | 0.503 | 0.111 |
| **$R^2$** | 0.728 | 0.682 | 0.828 | 0.793 | 0.768 | 0.824 |

As is shown, the highest regression coefficient values (0.99) are observed for the pseudo-second-order equation. In addition, the calculated adsorption capacities are close to those determined theoretically. Therefore, it is suggested that the adsorption of Cd and Mg ions on surface clays is chemical (Ho & McKay, 1999; Doğan & Alkan, 2003). Moreover, it was observed that the plots did not pass through the origin when the kinetic data was simulated using the intra-particular diffusion model, showing that intra-particular diffusion is not the only rate-limiting process for the two studied metal ions ($R^2$ values are less than 0.68). It was shown that the bigger the intercept, the more the surface adsorption contributed to the rate-limiting step. The C parameter depicts the boundary layer effect or surface adsorption.

*Isotherms Study*

To better understand the adsorption mechanism, the adsorption equilibrium data of Cd and Mg ions in the presence of the studied clays were simulated using Langmuir, Freundlich, Temkin, and Dubinin-Radushkevich models (Freundlich, 1906; Langmuir, 1918; Al-Ghouti *et al*., 2005; Al-Ghouti & Da'ana, 2020). **Table 3** summarizes the constant parameters for the different studied models.

**Table 3.** Relative constant parameters of Langmuir, Freundlich, Temkin, and Dubinin–Radushkevich models

| | Cd | | | Mg | | |
|---|---|---|---|---|---|---|
| | **BBC** | **ABC** | **ACHT(Ta)** | **BBC** | **ABC** | **ACHT(Ta)** |
| **Langmuir 1** | | | | | | |
| **$q_{max}$** | 78.125 | 113.636 | 45.454 | 0.507 | 0.888 | 0.35 |
| **$K_L$** | 0.007 | 0.004 | -0.006 | 5.29 | 11.5 | 5.076 |
| **$R^2$** | 0.708 | 0.427 | 0.525 | 0.998 | 0.999 | 0.999 |
| **Freundlich** | | | | | | |
| **$K_F$** | 0.815 | 0.723 | 0.489 | 0.552 | 0.765 | 0.515 |
| **1/n** | 0.914 | 0.963 | 0.882 | 0.779 | 0.749 | 0.696 |
| **$R^2$** | 0.987 | 0.985 | 0.991 | 0.97 | 0.98 | 0.98 |
| **Dubinin–Radushkevich** | | | | | | |
| **$q_s$** | 9.256 | 3.113 | 2.794 | 0.695 | 0.986 | 0.654 |
| **b** | $5.6710^{-6}$ | $6.0310^{-6}$ | $7.0910^{-6}$ | $3.4810^{-8}$ | $4.0410^{-8}$ | $4.1410^{-8}$ |
| **E** | 296.95 | 287.95 | 256.56 | 3790 | 3518 | 3475 |
| **$R^2$** | 0.952 | 0.96 | 0.949 | 0.825 | 0.985 | 0.998 |
| **Temkin** | | | | | | |
| **$A_T$** | $4.4\ 10^{-6}$ | $8.8\ 10^{-6}$ | $1.026\ 10^{-5}$ | 1.46 | 1.936 | 1.295 |
| **$B_T$** | 137.584 | 149.918 | 169.741 | 6080.448 | 3364.393 | 9027.144 |
| **$R^2$** | 0.995 | 0.995 | 0.98 | 0.985 | 0.967 | 0.994 |

The highest regression coefficient values are observed for both the Freundlich and Temkin equations. However, the adsorption of Mg could also follow the Langmuir model (Boughzala *et al*., 2020). The surface of the adsorbents is expected to undergo multilayer adsorption. For the Freundlich model, the values of n are higher than 1, indicating favorable adsorption. The Temkin constant values, $B_T$ related to the heat of sorption, varied between 137 J/mol and 149 J/mol, in the case of the adsorption of Cd ions which suggests physical adsorption. These constant values (3364 J/mol - 9027 J/mol) are much greater than those calculated for Cd ions. This suggests that the interaction between the clays and Mg ions is chemical (Al-Ghouti & Da'ana, 2020). Also, the high $R^2$ values observed for Radushkevich isotherm may suggest that the adsorption mechanism onto heterogeneous surfaces of the adsorbents varies with a Gaussian energy distribution (Saleh & Ali, 2018; Bembli *et al*., 2022). The results from the middle range of concentrations and high solute activity have frequently been well fit by the model. As globally observed, the adsorption phenomenon remains complex, and physical and chemical interactions are involved.

*Comparison of the Removal Performance with Other Reported Techniques*

To describe the performance of the current investigated technique, a comparison with other methods described in the literature was assessed. **Table 4** gives a comparison of the adsorption capacities

of $Cd^{2+}$ and $Mg^{2+}$ ions with other reported methods in the literature. For instance, the removal efficiency of $Cd^{2+}$ ions is considered significant compared to the literature (Yu & Liu, 2010; Khamar *et al*., 2021; Mahrou *et al*., 2021; Kouzbour *et al*., 2022; Samrane & Bouhaouss, 2022; Es-Said *et al*., 2023; Marszałek *et al*., 2023) and it is more important compared to the method utilizing precipitation by birnessite-type Na-$MnO_2$ (Amarray *et al*., 2023).

**Table 4.** Comparison of the adsorption capacities of $Cd^{2+}$ and $Mg^{2+}$ ions with other reported methods in the literature

| | **$Cd^{2+}$ ions** | | **$Mg^{2+}$ ions** | |
|---|---|---|---|---|
| Method | Removal (%) | Ref | Removal (%) | Ref |
| Current adsorbents | 55 | This study | 46 | This study |
| Adsorption using natural clays | 67 | (Al-Ghouti & Da'ana, 2020) | - | - |
| Precipitation by birnessite-type Na-$MnO_2$ | 35 | (Es-Said *et al*., 2023) | - | - |
| Precipitation using sulfide | 85 | (Kouzbour *et al*., 2022) | - | - |
| Precipitation using commercial anion exchange resins | 95 | (Marszałek *et al*., 2023) | | |
| Complexation by organic coordination ligands | 86 | (Samrane & Bouhaouss, 2022) | | |
| Precipitation using magnesium fluorosilicate | - | - | 85 | (Khamar *et al*., 2021) |
| Extraction using dinony lnaphthalene sulfonic acid | - | - | 97 | (Yu & Liu, 2010) |
| Precipitation | | | 75 | (Mahrou *et al*., 2021) |

## Conclusion

In this study, natural and activated clays were employed for the adsorption of Cd and Mg ions from $H_3PO_4$ solution. The studied clays were characterized using Elemental analysis, SEM, FT-IR spectroscopy, XRD, BET, and TGA-DTA. The studied clays were principally constituted of $SiO_2$ (43.64 - 51.24 %), and $Al_2O_3$ (19.92 – 31.24%). The specific surface area values of the studied clays ranged from 74.25.35 to 85.14 $m^2$/g. The XRD results showed the presence of kaolinite, quartz, goethite, and hematite. The clays were formed of agglomerates with irregular shapes and small sizes. The cadmium and magnesium retention capacity in clays are higher than 50% and 36%, respectively. Compared to results reported in the literature, the currently studied clays could be considered significant adsorbents for the removal of metal ions. The adsorption process complied well with the pseudo-second kinetic order and Freundlich isotherm equations. The process was chemical. Future investigations will be extended for the use of other natural minerals for the adsorption of pollutants.

**Acknowledgments:** None

**Conflict of interest:** None

**Financial support:** None

**Ethics statement:** None

## References

Al-Ghouti, M. A., & Da'ana, D. A. (2020). Guidelines for the use and interpretation of adsorption isotherm models: A review. *Journal of Hazardous Materials*, *393*, 122383-122405.

Al-Ghouti, M., Khraisheh, M. A. M., Ahmad, M. N. M., & Allen, S. (2005). Thermodynamic behaviour and the effect of temperature on the removal of dyes from aqueous solution using modified diatomite: A kinetic study. *Journal of Colloid and Interface Science*, *287*(1), 6-13.

Amarray, A., Salmi, M., Hlil, E. K., Dahbi, M., Khaless, K., Azzi, M., & Elghachtouli, S. (2023). Reduction of cadmium content in 29% and 54% P2O5 phosphoric acid by manganese oxide material birnessite-type Na-MnO2. *Desalination*, *560*, 116677.

Becker, P. (1989). *Phosphates & phosphoric acid: Raw materials, technology & economics of the wet process*, second ed., Marcel Dekker, New York.

Bembli, M., Khiari, R., Hidouri, M., & Boughzala, K. (2024). Structural and electric properties of lanthanide doped oxybritholites materials. *Chemistry Africa*, 1-18.

Bembli, M., Khiari, R., Kooli, F., & Boughzala, K. (2021). Investigation of basic blue 41 removal by waste product from the phosphate industry: Batch design and regeneration. *Desalin Water Treats*, *74*(2), 41-79.

Bembli, M., Kooli, F., Khiari, R., & Boughzala, K. (2022). Removal of basic blue 41 by waste product from the phosphate industry: Batch design and regeneration *Desalination and Water Treatment*, *246*, 291-303.

Bezzi, N., Merabet, D., Benabdeslem, N., & Arkoub, H. (2001). Caracterisation physico-chimique du minerai de phosphate de Bled El Hadba—Tebessa. In *Annales de Chimie Science des Matériaux* (Vol. 26, No. 6, pp. 5-23). No longer published by Elsevier.

Boughzala, K., & Hidouri, M. (2020). Elimination of acid red 88 by waste product from the phosphate industry: Batch design and regeneration. *Pathways and Challenges for Efficient Desalination*.

Boughzala, K., Kooli, F., Meksi, N., Bechrifa, A., & Bouzouita, K. (2020). Waste products from the phosphate industry as efficient removal of Acid Red 88 dye from aqueous solution: Their regeneration uses and batch design adsorber. *Desalination Water Treat*, *202*, 410-419.

Delcea, C., & Siserman, C. (2021). The emotional impact of Covid-19 on forensic staff. *Romanian Journal of Legal Medicine*, *29*(1), 142-146.

Delcea, C., Bululoi, A. S., Gyorgy, M., & Rad, D. (2023a). Psychological distress prediction based on maladaptive cognitive schemas and anxiety with random forest regression algorithm. *Pharmacophore*, *14*(5), 62-69.

Delcea, C., Bululoi, A. S., Gyorgy, M., & Siserman, C. V. (2023c). Medico-legal approach to incestuous sexual orientation in men. *Archives of Pharmacy Practice*, *14*(4-2023), 69-74.

Delcea, C., Rad, D., Gyorgy, M., Runcan, R., Breaz, A., Gavrilă-Ardelean, M., & Bululoi, A. S. (2023b). A network analysis approach to romanian resilience-coping mechanisms in the Covid-19 era. *Pharmacophore*, *14*(4), 57-63.

Doğan, M., & Alkan, M. (2003). Adsorption kinetics of methyl violet onto perlite. *Chemosphere*, *50*(4), 517-528.

Es-Said, A., El Hamdaoui, L., Ennoukh, F. E., Nafai, H., Zerki, N., Lamzougui, G., & Bchitou, R. (2023). Chemometrics approach for adsorption multi-response optimization of Cu (II), Zn (II), and Cd (II) ions from phosphoric acid solution using natural clay. *Phosphorus, Sulfur, and Silicon and the Related Elements*, *198*(5), 424-434.

European Commission. (2007). Reference document on best available techniques for the manufacture of large volume inorganic chemicals – Ammonia. Acids and Fertilizers. Sevilla, Spain.

Freundlich, H. M. F. (1906). Over the adsorption in solution. *The Journal of Physical Chemistry*, *57*, 385-470.

Gmati, N., Agougui, H., Hidouri, M., & Boughzala, K. (2022). Elaboration of strontium apatites doped with lanthanum and cesium by solid-state reaction and by mechanochemical synthesis. *Journal of Materials and Environmental Science*, *13*(06), 665.

Gonzalez, M. P., Navarro, R., Saucedo, I., Avila, M., Revilla, J., & Bouchard, C. (2002). Purification of phosphoric acid solutions by reverse osmosis and nanofiltration. *Desalination*, *147*(1-3), 315-320.

Ho, Y. S., & McKay, G. (1999). Pseudo-second order model for sorption processes. *Process Biochemistry*, *34*(5), 451-465.

Ho, Y. S., Chiang, T. H., & Hsueh, Y. M. (2005). Removal of basic dye from aqueous solution using tree fern as a biosorbent. *Process Biochemistry*, *40*(1), 119-124.

Inglezakis, V. J., Fyrillas, M. M., & Stylianou, M. A. (2018). Two-phase homogeneous diffusion model for the fixed bed sorption of heavy metals on natural zeolites. *Microporous and Mesoporous Materials*, *266*, 164-176.

Khamar, L., Kadiri, M. S., & Omari, L. (2021). Process for Reducing the magnesium content in industrial phosphoric acid by its precipitation to magnesium fluorosilicate. *RASAYAN Journal of Chemistry*, *14*(2), 836-843.

Kouzbour, S., Gourich, B., Gros, F., Vial, C., & Stiriba, Y. (2022). A novel approach for removing cadmium from synthetic wet phosphoric acid using sulfide precipitation process operating in batch and continuous modes. *Minerals Engineering*, *187*, 107809.

Kthiri, K., Mehnaoui, M., Hidouri, M., & Boughzala, K. (2022). Comparative evaluation of industrial phosphoric acids desulfation capabilities of limes and barium carbonate. *International Research Journal of Pure and Applied Chemistry*, *23*(2), 17-27.

Langmuir, I. (1918). The adsorption of gases on plane surfaces of glass, mica and platinum. *Journal of the American Chemical Society*, *40*(9), 1361-1403.

Mahrou, A., Jouraiphy, R., Mazouz, H., Boukhair, A., & Fahad, M. (2021). Magnesium removal from phosphoric acid by precipitation: Optimization by experimental design. *Chemical Industry and Chemical Engineering Quarterly*, *27*(2), 113-119.

Marszałek, M., Knapik, E., Piotrowski, M., & Chruszcz-Lipska, K. (2023). Removal of cadmium from phosphoric acid in the presence of chloride ions using commercially available anion exchange resins. *Journal of Industrial and Engineering Chemistry*, *118*(25), 488-498.

Saleh, T. A., & Ali, I. (2018). Synthesis of polyamide grafted carbon microspheres for removal of rhodamine B dye and heavy metals. *Journal of Environmental Chemical Engineering*, *6*(4), 5361-5368.

Samrane, K., & Bouhaouss, A. (2022). Highly selective complexation of cadmium from wet phosphoric acid by organic coordination ligands. *Minerals Engineering*, *189*, 107858.

Sboui, N., Agougui, H., Jabli, M., & Boughzala, K. (2022). Synthesis, physico-chemical, and structural properties of silicate apatites: Effect of synthetic methods on apatite structure and dye removal. *Inorganic Chemistry Communications*, *142*, 109628.

Toama, H. Z. (2017). World phosphate industry. *Iraqi Bulletin of Geology and Mining*, (7), 5-23.

Wang, H., Li, R., Fan, C., Feng, J., Jiang, S., & Han, Z. (2015). Removal of fluoride from the acid digestion liquor in production process of nitrophosphate fertilizer. *Journal of Fluorine Chemistry*, *180*, 122-129.

Yu, J., & Liu, D. (2010). Extraction of magnesium from phosphoric acid using dinonylnaphthalene sulfonic acid. *Chemical Engineering Research and Design*, *88*(5-6), 712-717.

Zhao, B., Xu, X., Xu, S., Chen, X., Li, H., & Zeng, F. (2017). Surface characteristics and potential ecological risk evaluation of heavy metals in the bio-char produced by co-pyrolysis from municipal sewage sludge and hazelnut shell with zinc chloride. *Bioresource Technology*, *243*, 375-383.